

Dynamics and Equilibrium of the Penetration of Soluble Cetyltrimethylammonium Bromide into Langmuir Monolayers of Arachidic Acid under Different pH Conditions

V. B. Fainerman,[†] D. Vollhardt,^{*,‡} A. Roth,[§] M. Fricke,[§] and D. Volkmer[§]

Medical Physicochemical Centre, Donetsk Medical University, 16 Ilych Avenue, Donetsk 83003, Ukraine, Max Planck Institute of Colloids and Interfaces, D-14424 Potsdam/Golm, Germany, and Faculty of Chemistry (AC1), University of Bielefeld, P.O. Box 100 131, D-33501 Bielefeld, Germany

Received: January 27, 2004; In Final Form: June 2, 2004

Experimental and theoretical studies of the equilibrium and dynamics of the penetration of the soluble cationic surfactant cetyltrimethylammonium bromide (CTAB) into arachidic acid monolayers are reported. The experimental studies of the system are performed at different pH values in acidic, alkaline, and neutral media. The penetration of CTAB from the alkaline subphase into the arachidic acid monolayer is shown to result in a significant increase of the surface pressure of the mixed monolayer, whereas the surface pressure jump for the penetration from the acidic subphase does not differ from that corresponding to the adsorption from the single CTAB solution with the same concentration onto the pure aqueous surface. This phenomenon is explained by the fact that the dissociation degrees of arachidic acid are different (the dissociation is the largest in the alkaline subphase, and nearly no dissociation exists in the acidic subphase), and in the alkaline subphase, strong Coulombic interaction exists between the CTA⁺ cation and the arachidate anion in the mixed monolayer. A new theoretical model is proposed involving the enthalpic nonideality of the mixed monolayer (the interaction between the insoluble and soluble monolayer components) which provides a quantitative interpretation of the experimental results with physically reasonable values of the model parameters.

Introduction

The equilibrium and dynamic behaviors of mixed monolayers consisting of soluble and insoluble amphiphiles at fluid–liquid interfaces play an important role in various processes and have been studied in numerous publications.^{1–9}

In recent reviews,^{10,11} an analysis is given of the main theoretical methods used for describing mixed monolayers, with special emphasis given to systems where the insoluble component of the monolayer is capable of two-dimensional condensation. In these cases, (i) phase transition and the corresponding condensation of the insoluble component affects essentially the adsorption behavior of the soluble amphiphile and (ii) the adsorption of the soluble component affects the 2D condensation of the insoluble species.

Most recently, it was shown that the dynamic formation of mixed monolayers at the oil–water interface can be utilized as a means of templating inorganic hierarchical materials of complex shapes, including star-shaped silica/titania shells which bear a striking resemblance to the natural shells of radiolaria.¹² The combination of amphiphilic molecules used in this study has led us to investigate the penetration kinetics of soluble cetyltrimethylammonium cations into insoluble monolayers of arachidic acid in more detail by varying the pH value and the CTA⁺ concentration of the aqueous subphase.

The penetration technique can be used to study the dynamic behavior of mixed monolayers consisting of a soluble and an insoluble amphiphile. During the penetration, first the insoluble

monolayer with some predefined coverage is formed, and then, the adsorption (penetration) dynamics of the soluble amphiphile into this monolayer is studied. It was particularly found that penetration of the soluble amphiphile results in the effect that the insoluble component starts to undergo condensation at a lower monolayer coverage as compared with that occurring in its pure Langmuir monolayer.^{9–11}

In the present study, we make an attempt to analyze the behavior of a mixed monolayer composed of the insoluble arachidic acid and the soluble cationic surfactant cetyltrimethylammonium bromide (CTAB) which penetrates into this monolayer. The experimental studies of this system were performed at different pH values in acidic, alkaline, and neutral media. The *dissociation degrees of the arachidic acid* monolayer on these media are different (with the maximum dissociation degree on the alkaline medium and nearly no dissociation on the acidic medium), and this has striking consequences on its phase behavior and structure features.^{13–16} Accordingly, CTAB penetration in the alkaline medium can result in strong Coulombic interaction between the CTA⁺ cation and the anionic arachidate in the mixed monolayer. This case was disregarded in our earlier theoretical approaches about the penetration of soluble surfactants into Langmuir monolayers.^{10,11}

In the present work, we generalize the theoretical models of the penetration equilibrium and dynamics with the focus on systems which exhibit a strong nonideality of the mixed monolayer and compare the theoretical results with the experimental data.

Theory

The equation of state and adsorption isotherm equation for the nonideal monolayer (with respect to both the enthalpy and

* Corresponding author.

[†] Donetsk Medical University.

[‡] Max-Planck Institute of Colloids and Interfaces.

[§] University of Bielefeld.

the entropy) of an insoluble (eq 1) and a soluble (eq 2) component have the following form:¹¹

$$\Pi = -\frac{RT}{\omega_0} \left[\ln(1 - \theta_1 - \theta_2) + \theta_1 \left(1 - \frac{1}{n_1}\right) + \theta_2 \left(1 - \frac{1}{n_2}\right) + a_1\theta_1^2 + a_2\theta_2^2 + a_{12}\theta_1\theta_2 \right] \quad (1)$$

$$b_2c_2 = \frac{\theta_2}{(1 - \theta_1 - \theta_2)^{n_2}} \exp(-2a_2\theta_2 - 2a_{12}\theta_1) \times \exp[(1 - n_2)(a_1\theta_1^2 + a_2\theta_2^2 + a_{12}\theta_1\theta_2)] \quad (2)$$

where R is the gas law constant, T is temperature, $\Pi = \gamma_0 - \gamma$ is the surface pressure, γ_0 and γ are the surface tension of the solvent and the solution, respectively, ω is the molar area, θ is the surface coverage, $\theta = \Gamma\omega$, Γ is the adsorption, c is the bulk concentration, a is the intermolecular interaction constant, b is the adsorption equilibrium constant, ω_0 is the molar area of the solvent, and $n_i = \omega_i/\omega_0$.

Note that eq 2 was obtained from the simultaneous solution of eq 1 and the Gibbs' adsorption equation. The two-dimensional solution model results in another adsorption isotherm equation for $n_i > 1$.¹⁷ However, with the assumption $\omega_0 = \omega_i$, the two models lead to the same adsorption isotherm equation. The convention $\omega_0 = \omega_i$ means that the entropic nonideality contribution to the activity coefficients vanishes.¹⁷ Therefore, for this case, eqs 1 and 2 can be reduced to the following equations:

$$\Pi = -\frac{RT}{\omega_0} [\ln(1 - \theta_1 - \theta_2) + a_1\theta_1^2 + a_2\theta_2^2 + a_{12}\theta_1\theta_2] \quad (3)$$

$$b_2c_2 = \frac{\theta_2}{(1 - \theta_1 - \theta_2)} \exp(-2a_2\theta_2 - 2a_{12}\theta_1) \quad (4)$$

The equations of state (eqs 1 and 3) have the logarithmic form for both components which often disagrees with the experimental results for insoluble monolayers.^{10,11} For these systems, Volmer's or van der Waals' equations of state are more appropriate.

In the phase coexistence region ($A < A_c$), the generalized Volmer's equation has the following form:^{18,19}

$$\Pi = \frac{kT\alpha\beta}{A - \omega[1 + \epsilon(\alpha\beta - 1)]} - \Pi_{\text{coh}} \quad (5)$$

where k is the Boltzmann constant, ω is the partial molecular area for monomers (or the limiting area of a molecule in the gaseous state), A is the area per molecule, A_c is the molecular area which corresponds to the onset of the phase transition (i.e., at $\Pi = \Pi_c$), and Π_{coh} is the cohesion pressure, which accounts for the intermolecular interaction. The parameter α expresses the dependence of the aggregation constant on the surface pressure:

$$\alpha = \frac{A}{A_c} \exp\left[-\epsilon \frac{\Pi - \Pi_c}{kT} \omega\right] \quad (6)$$

and β is the fraction of the monolayer free from aggregates:

$$\beta = 1 + \omega(1 - \epsilon)(\alpha - 1)/A \quad (7)$$

where $\epsilon = 1 - \omega_{\text{cl}}/\omega$, ω_{cl} is the area per monomer in a cluster

$$\omega_{\text{cl}} = \omega(1 - \epsilon) = \omega(1 - \epsilon_0 - \eta\Pi) \quad (8)$$

ϵ_0 is the relative jump of the area per molecule, and η is the relative two-dimensional compressibility of the condensed monolayer.²⁰

To account for the influence of the adsorption of a soluble amphiphile on the surface pressure of the mixed monolayer, one has to subtract from eq 3 the surface pressure of the insoluble monolayer component:

$$\Pi = -\frac{RT}{\omega_0} [\ln(1 - \theta_1) + a_1\theta_1^2] \quad (9)$$

thus obtaining the net effect of the penetration of the soluble amphiphile into the insoluble monolayer, that is, the variation (jump) $\Delta\Pi$ of the mixed monolayer surface pressure:

$$\Delta\Pi = -\frac{RT}{\omega_0} [\ln(1 - \theta_2/(1 - \theta_1)) + a_2\theta_2^2 + 2a_{12}\theta_1\theta_2] \quad (10)$$

It could be assumed that eq 10 is applicable not only to the case when the equation of state (eq 9) is used to describe the behavior of the insoluble monolayer but also to any other equation of state valid for the insoluble component, in particular, eq 5.

It is seen from eq 4 that, if the parameter a_{12} which corresponds to the intermolecular interaction between the components of the insoluble and soluble components is large, then, at a high enough coverage of the monolayer by the insoluble component, θ_1 , the monolayer coverage by the soluble amphiphile, θ_2 (at its fixed concentration in the solution), becomes essentially higher, as $\exp(-2a_{12}\theta_1) < 1$. Then, it follows from eq 10 that under these conditions the $\Delta\Pi$ value can also become much higher.

In contrast, it is seen from eqs 4 and 10 that for the ideal monolayer the $\Delta\Pi$ value does not depend on θ_1 and is determined by the following expression:¹¹

$$\Delta\Pi = (RT/\omega_0) \ln(1 + b_2c_2) \quad (11)$$

From eq 11, it follows that the variation (jump) of the surface pressure of the monolayer, which arises due to the adsorption of soluble surfactant, does not depend on θ_1 but depends on the value of b_2c_2 only. Under these conditions (as opposed to the case $a_{12} > 0$), an increase of θ_1 can result only in a decrease of the adsorption of the soluble surfactant.¹¹

$$\Gamma_2 = \frac{1 - \theta_1}{\omega_0} \frac{b_2c_2}{1 + b_2c_2} \quad (12)$$

According to eq 12, the monolayer coverage by the soluble component in the presence of the insoluble component decreases proportionally to $(1 - \theta_1)$. Therefore, the nonideality of the mixed monolayer enthalpy can significantly affect the dependencies of $\Delta\Pi$ and θ_2 on θ_1 , as demonstrated below.

To analyze the penetration kinetics of component 2 into the insoluble monolayer, and the variation in the surface pressure jump rate, $\Delta\Pi_t$, determined by this penetration process, the integrodifferential equation derived by Ward and Tordai²¹ was used, which represents the most general relationship between the dynamic adsorption, $\Gamma_2(t)$, and the subsurface concentration, $c_2(0, t)$, for fresh nondeformed surfaces:

$$\Gamma_2(t) = 2\sqrt{\frac{D_2}{\pi}} \left[c_2\sqrt{t} - \int_0^{\sqrt{t}} c_2(0, t - \lambda) d\sqrt{\lambda} \right] \quad (13)$$

where D_2 is the diffusion coefficient, t is time, and λ is a dummy

integration variable. For pure diffusion-controlled adsorption mechanisms, the adsorption isotherm (eq 4) is an additional equation between the adsorption and the subsurface concentration. The calculations with eqs 4, 10, and 13 were performed using the software package developed by E. Aksenenko²² and recently modified by this author to implement the formulation of the system studied here.

Experimental Section

Materials. Arachidic acid (eicosanoic acid; $\geq 99\%$ purity; from Merck Darmstadt, Germany) and cetyltrimethylammonium bromide (CTAB, hexadecyltrimethylammonium bromide; $\geq 99\%$ purity; from Fluka Buchs SG, Switzerland) were used as received. Trichloromethane was purchased from J. T. Baker (p.a. grade). An 8–10 μL portion of a solution of arachidic acid in trichloromethane (10 mg in 10 mL) was spread. The experiments were performed with acidic (0.01 M HCl), alkaline (0.01 M NaOH), and neutral (0.1 M NaCl) aqueous subphases. The distilled water was made ultrapure by a Milli-Q system.

Methods and Procedure. The principle of the penetration experiments is based on the idea that in a two-compartment trough a Langmuir monolayer, enclosed between two movable barriers and kept at selected conditions, can be swept over two subphases of different compositions. All penetration experiments were performed using a computer-controlled Nima 102MC film balance. The rectangular Teflon trough ($15 \times 7 \text{ cm}^2$) subdivided into two compartments is equipped with two barriers which can be moved in a coupled fashion or independently of one another. In the present work, the arachidic acid monolayer was spread between the barriers at the surface of one compartment filled with the corresponding (acidic, alkaline, or neutral) subphase, whereas the other compartment was filled with the CTAB solution of the same composition. Thus, the pure arachidic acid monolayer and the adsorption kinetics of the CTAB solution can be characterized independently of one another. Afterward, the arachidic acid monolayer was brought to the desired state, that is, molecular area, and swept onto the region containing the CTAB solution. Here, the penetration kinetics of the adsorbed CTAB into the arachidic acid monolayer can be studied. The same procedure for the characterization of the adsorption kinetics of CTAB at the surface of water was used, but in this case, no arachidic acid was spread between the two barriers of the first compartment.

Results and Discussion

The experimental surface pressure–area (Π – A) isotherms related to the area per one molecule of insoluble arachidic acid spread on neutral, acidic (0.01 M HCl), and alkaline (0.01 M NaOH) subphases are shown in Figure 1. After spreading both in the neutral medium and in the acidic medium, the arachidic acid monolayer is already at zero pressure in the two-phase coexistence region between the fluid and the condensed phases over the accessible temperature range. On the contrary, arachidic acid becomes ionized in alkaline medium, and therefore, it is less capable of aggregation to the condensed phase. Consequently, at room temperature, the quite wide coexistence range between the fluid and the condensed phases occurs first at $\Pi > 0 \text{ mN/m}$. In Figure 1, the area per molecule for the onset of the phase transition is outside the abscissa scale. The experimental Π – A isotherm for the alkaline subphase is matched quite well by eqs 5–8 for the following values of the model parameters: $A_c = 0.912 \text{ nm}^2$, $\omega = 0.24 \text{ nm}^2$, $\Pi_{\text{coh}} = 4.11 \text{ mN/m}$, and $\eta = 0.005 \text{ mN/m}$.

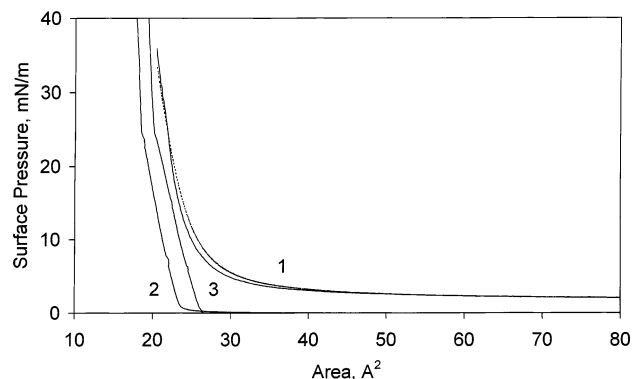


Figure 1. Experimental Π – A isotherms for the arachidic acid at different subphases: alkaline (1), acidic (2), and neutral (3). The theoretical curve (dotted line) for the alkaline subphase is calculated from the model of eqs 5–8. The parameter values are discussed in the text.

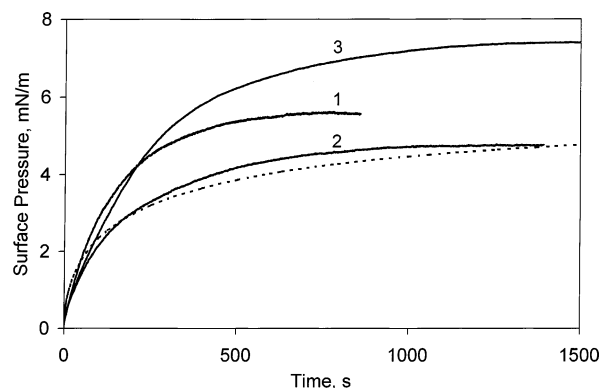


Figure 2. Experimental curves of the dynamic surface tension of 0.011 mM CTAB solutions (solid lines) in the alkaline subphase (curve 1), the acidic subphase (curve 2), and in the neutral subphase with the addition of 0.1 M NaCl (curve 3). The theoretical curve (dotted line) is calculated from the diffusion model (eq 13). The parameter values are discussed in the text.

In Figure 2, the surface pressure change during the adsorption of 0.011 mM CTAB solution in the acidic and alkaline media and also in the neutral medium with the addition of 0.1 M NaCl are shown. These results agree well with the general adsorption behavior of ionic surfactants.²³ For instance, the addition of salt leads to an increase of the adsorption activity of the ionic surfactant.

The theoretical curve of Figure 2, which describes quite satisfactorily the experimental results obtained for the 0.01 M HCl or 0.01 M NaOH subphases, was calculated from eq 13 and the relevant Frumkin's equations of state and the adsorption isotherm²³ for the single surfactant with the following parameter values: $\omega_0 = 1.32 \times 10^5 \text{ m}^2/\text{mol}$, $a_2 = 0$, $b_2 = 3.7 \times 10^4 \text{ L/mol}$, and $D_2 = 10^{-10} \text{ m}^2/\text{s}$. Note that for ionic surfactants $\omega_0 = \omega/2$.²³ Comparing these parameters of the CTAB adsorption isotherm with those reported in ref 24 for CTAB solutions in a neutral medium, one can see that the ω_0 and a_2 values above are virtually the same as those found in ref 24; only the b_2 value obtained in the present study is essentially higher as compared with the value $b_2 = 5.6 \times 10^3 \text{ L/mol}$ of ref 24.

This fact can be attributed to the presence of OH^- and Cl^- counterions in the alkaline and acidic media, respectively, which results in an increase of the CTAB adsorption activity.

Using the values obtained for the CTAB adsorption parameters, consider now the general penetration behavior which follows from eqs 4, 10, and 13 assuming enthalpic nonideality of mixed monolayers. Figure 3 illustrates the dependence of

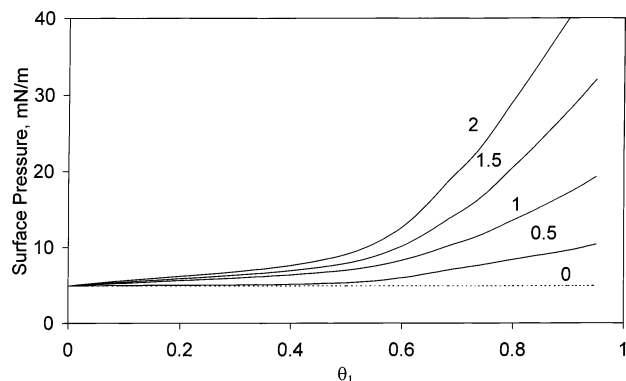


Figure 3. Correlation between the penetration equilibrium pressure, $\Delta\Pi$, and the surface coverage by the insoluble component, θ_1 , at the adsorption of a 0.011 mM CTAB solution for different a_{12} values (marked by the values at the curves).

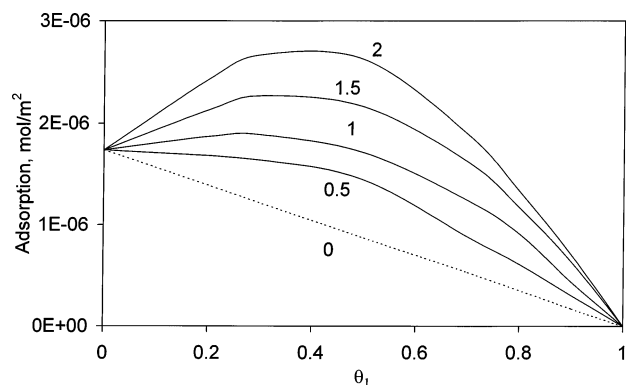


Figure 4. Correlation between the adsorption of the soluble component and the surface coverage by the insoluble component, θ_1 , at the adsorption of a 0.011 mM CTAB solution for different a_{12} values (marked by the values at the curves).

the surface pressure jump, $\Delta\Pi$, resulting from the penetration of the soluble component in equilibrium, on the monolayer coverage of the insoluble component, θ_1 . Here, for a 0.011 mM CTAB solution, the value of the nonideality parameter a_{12} was varied. It is seen that, whereas for the ideal monolayer the $\Delta\Pi$ value does not depend on θ_1 (as follows from eq 11), for the nonideal monolayers the $\Delta\Pi$ value increases sharply as θ_1 increases, and the higher the a_{12} value, the larger this increase.

Figure 4 represents the dependence of the penetration (adsorption) of the soluble component on θ_1 . In contrast to the ideal monolayer, for which the adsorption decreases linearly as θ_1 increases, this dependence is extreme for nonideal monolayers. According to eq 4, for nonideal monolayers, the higher the a_{12} value, the higher the adsorption. It is interesting to note that, for values of $a_{12} > 0.5$, a maximum exists in the dependence of the adsorption of the soluble component on θ_1 . The experimental dependencies of the kinetics of CTAB (concentration, 0.011 mM) penetration into the arachidic acid monolayer in various subphases and for different values of the area per one arachidic acid molecule are shown in Figures 5–7. It is seen that, in alkaline media, the penetration equilibrium pressure becomes significantly larger (as compared either with the acidic medium or with that characteristic for both media when the arachidic acid monolayer is absent), and the time necessary to attain this equilibrium value becomes lower. For example, for an area per one acid molecule of 0.5 nm² ($\theta_1 = 0.5$ –0.6), the equilibrium jump pressure value is $\Delta\Pi = 23$ mN/m (see Figure 5), which is ~ 4 times higher than that in the case when the monolayer is absent (see Figure 2). For still lower values of the area per one arachidic acid molecule of 0.4 and

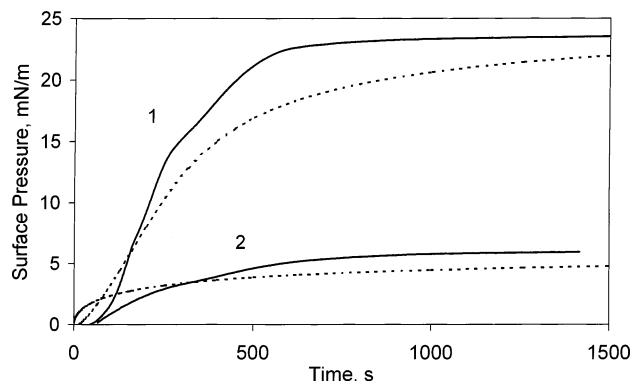


Figure 5. Dynamics of CTAB penetration into an arachidic acid monolayer ($A = 0.5$ nm², $c_2 = 0.011$ mM) in the alkaline (curve 1) and acidic (curve 2) subphases (solid lines). The theoretical curve (dotted lines) for the acidic subphase is taken from Figure 2, and that for the alkaline subphase is calculated from the model of eqs 4, 10, and 13 with $\theta_1 = 0.64$ and $a_{12} = 2.9$.

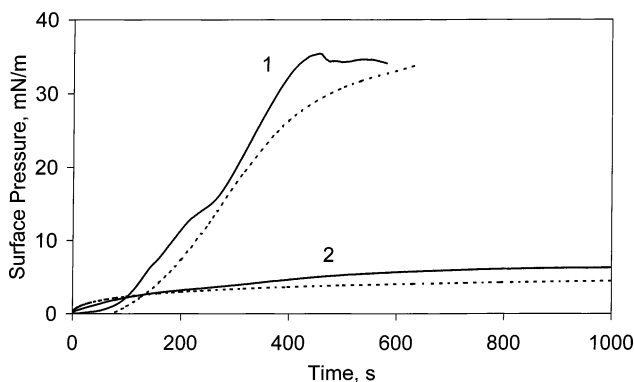


Figure 6. Dynamics of CTAB penetration into an arachidic acid monolayer ($A = 0.4$ nm², $c_2 = 0.011$ mM) in the alkaline (curve 1) and acidic (curve 2) subphases (solid lines). The theoretical curve (dotted lines) for the acidic subphase is taken from Figure 2, and that for the alkaline subphase is calculated from the model of eqs 4, 10, and 13 with $\theta_1 = 0.71$ and $a_{12} = 3.1$.

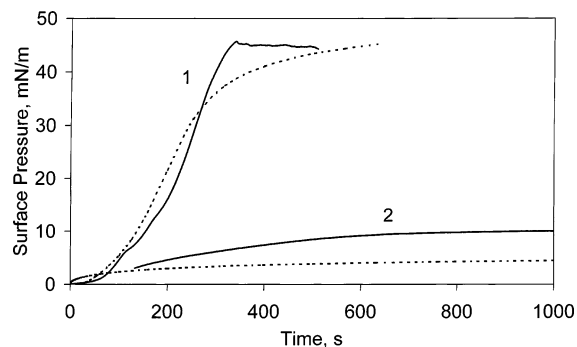


Figure 7. Dynamics of CTAB penetration into an arachidic acid monolayer ($A = 0.3$ nm², $c_2 = 0.011$ mM) in the alkaline (curve 1) and acidic (curve 2) subphases (solid lines). The theoretical curve (dotted lines) for the acidic subphase is taken from Figure 2, and that for the alkaline subphase is calculated from the model of eqs 4, 10, and 13 with $\theta_1 = 0.76$ and $a_{12} = 3.3$.

0.3 nm², which correspond to an increase of θ_1 to values of 0.65–0.7 and 0.75–0.8, respectively, the $\Delta\Pi$ values in the alkaline medium become higher: 35 and 45 mN/m, respectively (see Figures 6 and 7). With regard to the data presented in Figures 3 and 4, this increase of $\Delta\Pi$ can be ascribed to a significant increase of intermolecular interactions in the monolayer between the molecules of arachidic acid and CTAB in the presence of the alkaline subphase, when the a_{12} values are at the order of 2 or 3. This fact is quite understandable, because

in alkaline medium arachidic acid is completely dissociated, and the arachidate anion is capable of the formation of a neutral complex with the surface active cation CTA^+ in the surface layer. On the contrary, it is seen from Figures 5–7 that in acidic medium the equilibrium $\Delta\Pi$ value almost does not depend on the area occupied by the arachidic acid in the monolayer, which, according to eq 11, indicates that the behavior of the mixed monolayer is nearly ideal, corresponding to the value $a_{12} \cong 0$.

The experimental results agree quite well with the calculations of the penetration dynamics using the proposed model. All theoretical $\Delta\Pi$ – t curves for the acidic subphase in Figures 5–7 are those presented in Figure 2; that is, these curves were calculated for $a_{12} \cong 0$. It should be noted that the CTAB adsorption influences the contribution of arachidic acid to the surface pressure not only via the coefficient a_{12} (see the last term in eq 10) but also via the θ_{12} value. It follows from eqs 5 and 8 that the increase of the surface pressure caused by the CTAB adsorption leads to a decrease of ω_c (as $\eta = 0.005$ m/mN) and, therefore, to a slight decrease of θ_1 . This fact was neglected in the calculations illustrated by Figures 5–7. It is seen that only for closely packed arachidic acid monolayers (see Figure 7) an appreciable difference between the theoretical and experimental curves exists, which, however, can be eliminated if the nonideality parameter value $a_{12} \cong 0.7$ is introduced. In the case of the alkaline subphase, for the calculations of the $\Delta\Pi$ – t dependence, the adsorption characteristics for CTAB are taken to be those listed above ($\omega_0 = 1.32 \times 10^5$ m²/mol, $a_2 = 0$, $b_2 = 3.7 \times 10^4$ L/mol, and $D_2 = 10^{-10}$ m²/s) and the additional model parameters a_{12} and θ_1 were fitted. It is essential to note that the θ_1 values used in the calculations are quite close to the values of ω/A for the individual monolayer ($\theta_1 = 0.64$, 0.71, and 0.77 for $A = 0.5$ nm² ($\omega/A = 0.5$), $A = 0.4$ nm² ($\omega/A = 0.6$), and $A = 0.3$ nm² ($\omega/A = 0.8$), respectively), and the a_{12} values are found to be rather independent of θ_1 ; $a_{12} = 2.9$ – 3.3 throughout the studied range of the area per one arachidic acid molecule. This fact supports the physical validity of the model proposed. Some differences between the calculated θ_1 values and the values of ω/A used in the calculations can possibly be ascribed to the influence of the CTAB adsorption, which was neglected here. The values of nonideality (Frumkin's) parameters of 2 and above are critical for one-component monolayers of the nonionized surfactants, suggesting aggregation of monomers in this case.²⁴

Conclusion

Experimental and theoretical studies of the equilibrium and dynamics of the penetration of the soluble cationic surfactant CTAB into arachidic acid monolayers are reported. The experimental studies of the system were performed at different pH values in acidic, alkaline, and neutral media. The penetration of CTAB from the alkaline subphase is shown to result in a significant increase of the surface pressure of the mixed monolayer, whereas the surface pressure jump for the penetration from the acidic subphase does not differ from the adsorption

of CTAB molecules at the pure air–water interface under the same conditions. This phenomenon can be explained by the fact that the dissociation degree of arachidic acid is different (the dissociation is largest in the alkaline subphase and can be neglected in the acidic medium), and in the alkaline subphase, strong Coulombic interaction exists between the CTA^+ cation and the arachidate anion in the mixed monolayer. A theoretical model is developed involving the enthalpic nonideality of the mixed monolayer (interaction between the insoluble and soluble monolayer components) that provides quantitative interpretation of the experimental results with physically reasonable values of the model parameters.

Acknowledgment. D. Volkmer thanks the Deutsche Forschungsgemeinschaft (DFG grant Vo829/2) and the Volkswagen-Stiftung for financial support.

References and Notes

- (1) Pethica, B. A. *Trans. Faraday Soc.* **1955**, *51*, 1402.
- (2) McGregor, M. A.; Barnes, G. T. *J. Colloid Interface Sci.* **1976**, *54*, 439; **1977**, *60*, 408.
- (3) Motomura, K.; Hayami, I.; Aratono, M.; Matuura, R. *J. Colloid Interface Sci.* **1982**, *87*, 333.
- (4) Panaiotov, I.; Ter-Minassian-Saraga, L.; Albrecht, G. *Langmuir* **1985**, *1*, 395.
- (5) Hall, D. G. *Langmuir* **1986**, *2*, 809.
- (6) Tajima, K.; Koshinuma, M.; Nakamura, A. *Langmuir* **1991**, *7*, 2764.
- (7) Jiang, Q.; O'Lenick, C. J.; Valentini, J. E.; Chiev, I. C. *Langmuir* **1995**, *11*, 1138.
- (8) Sundaram, S.; Ferri, J. K.; Vollhardt, D.; Stebe, K. J. *Langmuir* **1998**, *14*, 1208.
- (9) Fainerman, V. B.; Makievski, A. V.; Vollhardt, D.; Siegel, S.; Miller, R. *J. Phys. Chem. B* **1999**, *103*, 330.
- (10) Vollhardt, D.; Fainerman, V. B. *Adv. Colloid Interface Sci.* **2000**, *86*, 103.
- (11) Fainerman, V. B.; Vollhardt, D. In *Organized Monolayers and Assemblies: Structure, Processes and Function*; Möbius, D., Miller, R., Eds.; Studies in Interface Science 15; Elsevier: Amsterdam, The Netherlands, 2002; pp 105–160.
- (12) Volkmer, D.; Tugulu, S.; Fricke, M.; Nilsen, T. *Angew. Chem.* **2003**, *115*, 60; *Angew. Chem., Int. Ed.* **2003**, *42*, 58.
- (13) Johann, R.; Vollhardt, D. *Mater. Sci. Eng., C* **1999**, *8–9*, 35.
- (14) Johann, R.; Brezesinski, G.; Vollhardt, D.; Möhwald, H. *J. Phys. Chem. B* **2001**, *105*, 2957.
- (15) Fainerman, V. B.; Vollhardt, D.; Johann, R. *Langmuir* **2000**, *16*, 7731.
- (16) Johann, R.; Vollhardt, D.; Möhwald, H. *Colloids Surf., A* **2001**, *182*, 313.
- (17) Fainerman, V. B.; Lucassen-Reynders, E. H.; Miller, R. *Adv. Colloid Interface Sci.* **2003**, *106*, 237; *Colloids Surf., A* **1998**, *143*, 141.
- (18) Fainerman, V. B.; Vollhardt, D. *J. Phys. Chem. B* **1999**, *103*, 145.
- (19) Vollhardt, D.; Fainerman, V. B.; Siegel, S. *J. Phys. Chem. B* **2000**, *104*, 4115.
- (20) Fainerman, V. B.; Vollhardt, D. *J. Phys. Chem. B* **2003**, *107*, 3098.
- (21) Ward, A. F. H.; Tordai, L. *J. Chem. Phys.* **1946**, *14*, 453.
- (22) Aksenenko, E. V. In *Surfactants: Chemistry, Interfacial Properties, Applications*; Fainerman, V. B., Möbius, D., Miller, R., Eds.; Studies in Interface Science 13; Elsevier: Amsterdam, The Netherlands, 2001; p 619.
- (23) Fainerman, V. B.; Lucassen-Reynders, E. H. *Adv. Colloid Interface Sci.* **2002**, *96*, 295.
- (24) Fainerman, V. B.; Miller, R.; Aksenenko, E. V.; Makievski, A. V. In *Surfactants—Chemistry, Interfacial Properties and Application*; Fainerman, V. B., Möbius, D., Miller, R., Eds.; Studies in Interface Science 13; Elsevier: Amsterdam, The Netherlands, 2001; p 189.